ATLAS/CMS 探测器简介

朱宏博
中国科学院高能物理研究所

课程内容安排

- 探测器总体设计 （课程 I）
- 径迹探测系统（课程 II）
- 量能器系统（课程 III）
- 缪子探测器系统（课程 IV）

课程 I

探测器总体设计

大型强子对撞机（LHC）

- 位于瑞士-法国边境，隧道总长27公里。设计质心能量为14 TeV （质子-质子对撞），瞬时亮度可至10^{34} $cm^{-2}s^{-1}$。
- LHC上的主要实验及其探测器：**ATLAS/CMS**（通用探测器），**LHCb**（B物理）和 **ALICE**（重离子对撞）

LHC 运行计划

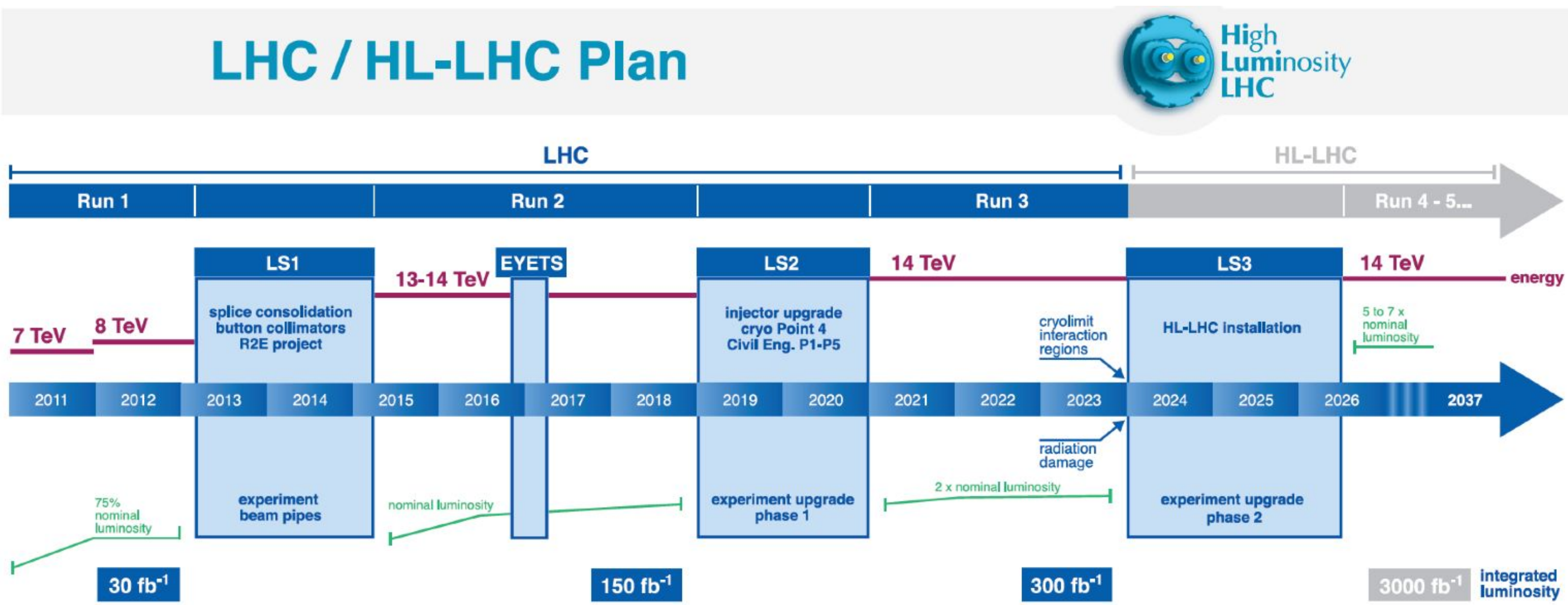

- LHC 2008(10)年启动，2011年运行在质心能量7 TeV，积分亮度约5 fb^{-1}；2012年运行在8 TeV，积分亮度约25 fb^{-1}；
- 2015年再次启动，运行质心能量13 TeV（再至14 TeV），瞬时亮度将至设计值10^{34} $cm^{-2}s^{-1}$。
- LS1 (Phase-0) → LS2 (Phase-I) → LS3 (Phase-II)，加速器、探测器等维护和升级。技术不断演化，提高，周期数十年。

设计物理目标

- 发现Higgs粒子 ✔
- 发现超对称粒子/新物理 （...）
- 标准模型精确测量 ✔

物理目标以及束流环境驱动探测器设计

TABLE 1 For a variety of physics processes expected to be the most abundantly produced at the LHC, expected numbers of events recorded by ATLAS and CMS for an integrated luminosity of 1 fb^{-1} per experiment

Physics process	Number of events per 1 fb^{-1}
QCD jets with $E_T > 150$ GeV	10^6 (for 10% of trigger bandwidth)
$W \to \mu\nu$	7.0×10^6
$Z \to \mu\mu$	1.1×10^6
$tt \to e/\mu + X$	1.6×10^5
Gluino-gluino production (of mass approximately 1 TeV)	10^2 to 10^3

ATLAS/CMS 探测器

ATLAS

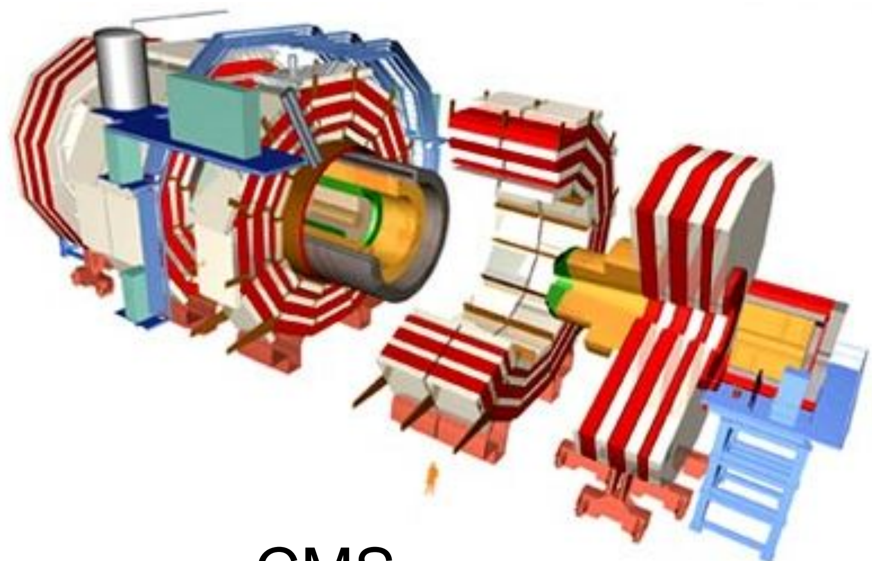

CMS

- 广泛的物理计划，探测器设计尽可能采用**不同设计理念以及不同技术**，从而降低LHC项目整体风险，并且可以相互验证实验结果（例如发现Higgs）。

主要设计参数

TABLE 2 Main design parameters of the ATLAS and CMS detectors

Parameter	**ATLAS**	**CMS**
Total weight (tons)	7000	12,500
Overall diameter (m)	22	15
Overall length (m)	46	20
Magnetic field for tracking (T)	2	4
Solid angle for precision measurements ($\Delta\phi \times \Delta\eta$)	$2\pi \times 5.0$	$2\pi \times 5.0$
Solid angle for energy measurements ($\Delta\phi \times \Delta\eta$)	$2\pi \times 9.6$	$2\pi \times 9.6$
Total cost (million Swiss francs)	550	550

探测器基本结构

- **内层**（靠近对撞点）：径迹探测器位于螺线管磁场内，精确测量从对撞点出发的各类带电粒子的动量；

↓

- **中间层**：电磁量能器和强子量能器吸收并测量电子、光子和强子的能量；

↓

- **外层**：缪子探测器以测量高能缪子（穿透量能器）的动量

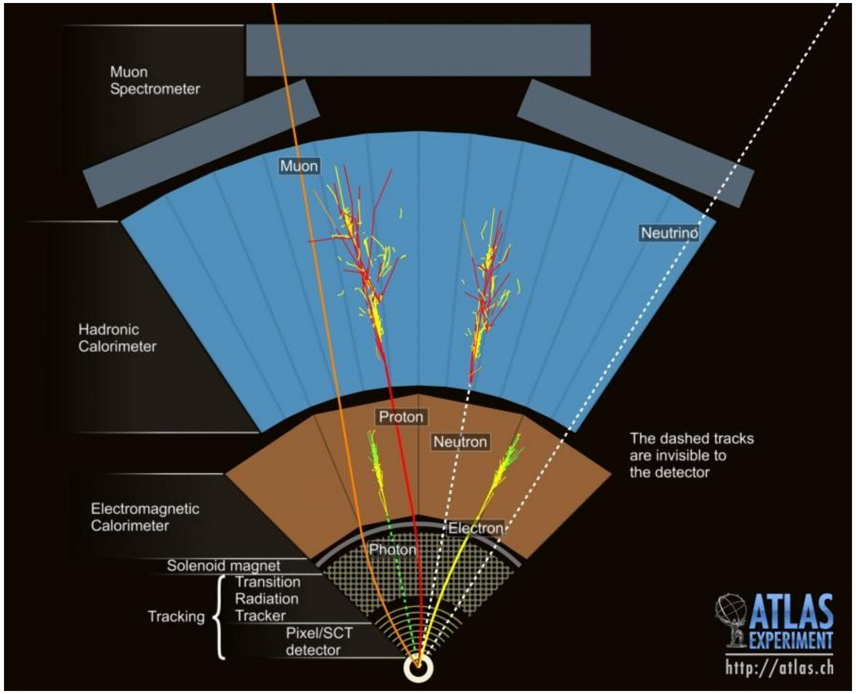

通用型探测器结构基本类似，具体布局和实现方法有差异，

各部分子探测器会进一步介绍

ATLAS谱仪磁场

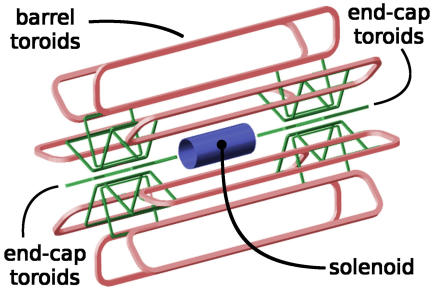

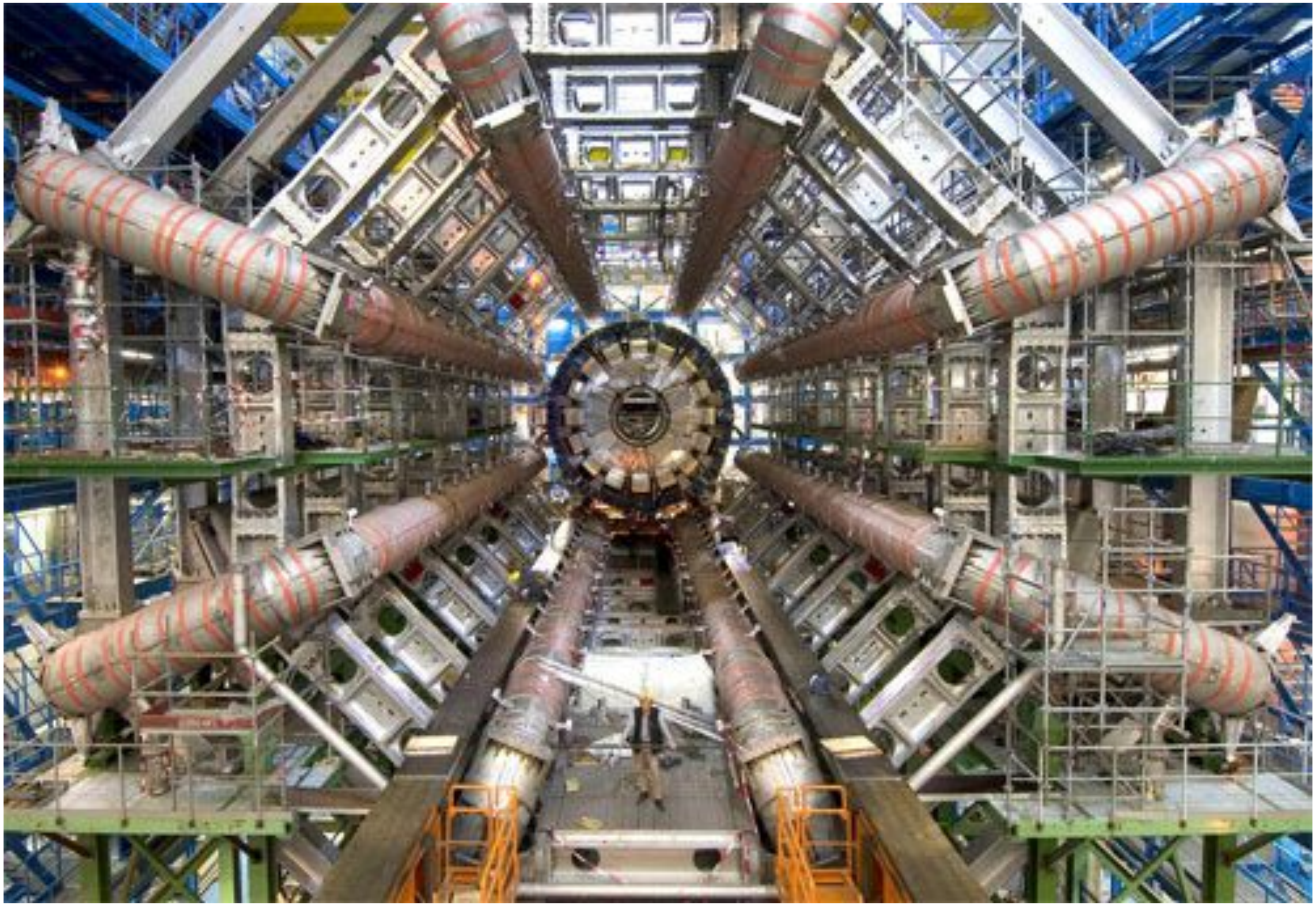

谱仪磁场参数对比

TABLE 3 Main parameters of the CMS and ATLAS magnet systems

	CMS	ATLAS		
Parameter	**Solenoid**	**Solenoid**	**Barrel toroid**	**End-cap toroids**
Inner diameter	5.9 m	2.4 m	9.4 m	1.7 m
Outer diameter	6.5 m	2.6 m	20.1 m	10.7 m
Axial length	12.9 m	5.3 m	25.3 m	5.0 m
Number of coils	1	1	8	8
Number of turns per coil	2168	1173	120	116
Conductor size (mm^2)	64×22	30×4.25	57×12	41×12
Bending power	$4\ T \cdot m$	$2\ T \cdot m$	$3\ T \cdot m$	$6\ T \cdot m$
Current	19.5 kA	7.7 kA	20.5 kA	20.0 kA
Stored energy	2700 MJ	38 MJ	1080 MJ	206 MJ

谱仪磁场优劣

1. The higher field strength and uniformity of the CMS solenoid provide better momentum resolution and better uniformity over the full η-coverage for the inner tracker (see Section 3). CMS 强均匀磁场，利于提高动量分辨率
2. The position of the ATLAS solenoid just in front of the barrel ECAL limits to some extent the energy resolution in the region $1.2 < |\eta| < 1.5$ (see Section 4). ATLAS 磁场位置降低特定位置电磁量能器能量分辨率
3. The position of the CMS solenoid outside the calorimeter limits the number of interaction lengths available to absorb hadronic showers in the region $|\eta| < 1$ (see Section 4). CMS 磁场位于量能器外层，限制作用长度
4. The muon spectrometer system in ATLAS provides an independent and high-accuracy measurement of muons over the full η-coverage required by the physics. This requires, however, an alignment system with specifications an order of magnitude more stringent (few tens of micrometers) than those of the CMS muon spectrometer (see Section 5). In addition, the magnetic field in the ATLAS muon spectrometer must be known to an accuracy of a few tens of Gauss over a volume of nearly 20,000 m^3. The software implications of these requirements are nontrivial (size of map in memory, access time). ATLAS 磁场允许独立测量，精度要求高
5. The muon spectrometer system in CMS has limited stand-alone measurement capabilities, and this affects the triggering capabilities for the luminosities envisaged for the LHC upgrade. CMS 缪子探测器触发有限

触发系统

- 为什么需要触发？

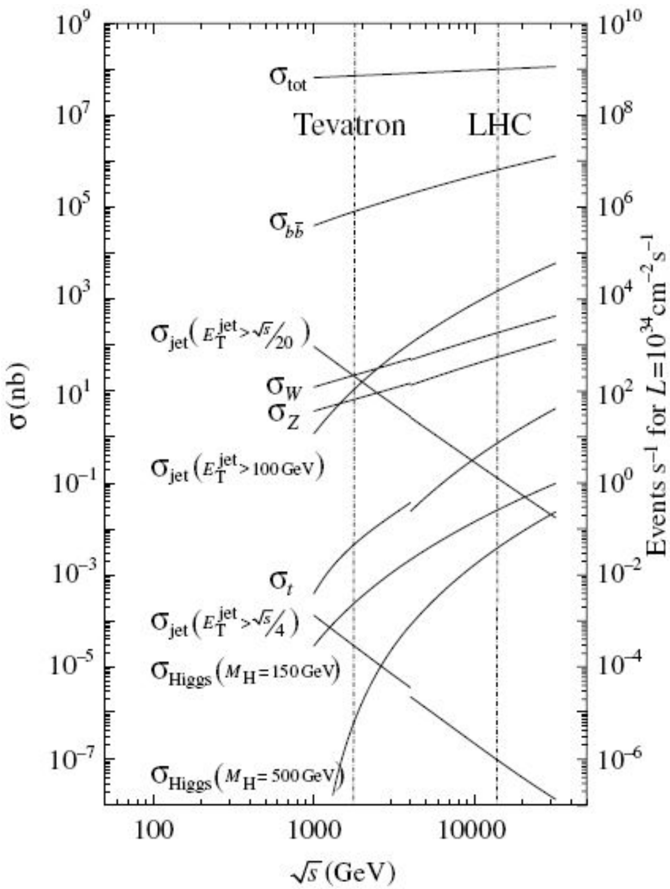

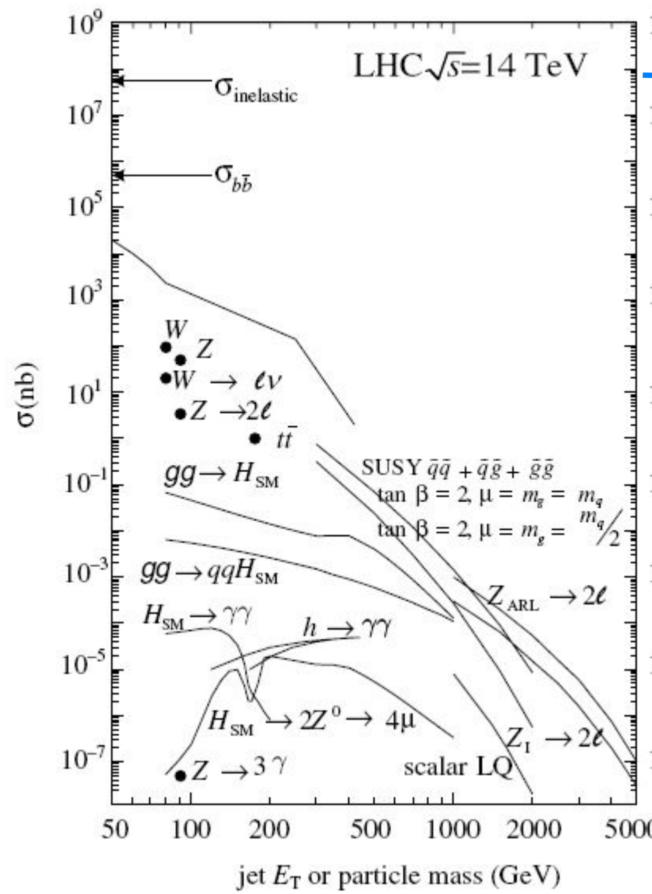

事例率 10^9

硬件、软件事例选择

存储率 10^2（感兴趣的物理事例）

触发系统基本要求

1. To provide enough bandwidth and computing resources, within financial constraints, to minimize the dead time at any luminosity while maintaining the maximum possible efficiency for the discovery signals. The current goal is a total dead time of less than a few (1–2) percent. Most of this dead time is currently planned to occur in the Lvl-1 trigger.
2. To be robust, i.e., provide an operational efficiency that does not depend significantly on the noise and other conditions in the detector or on changes with time of the calibration and detector alignment constants.
3. To provide the possibility of validating and of computing the overall selection efficiencies using the data only, with as little reference to simulation as possible. This implies usage of multiple trigger requirements with overlapping thresholds.
4. To uniquely identify the bunch crossing that gave rise to the trigger.
5. To allow for the readout, processing, and storage of events needed for calibration purposes.

触发系统基本要求

What is different in the two experiments is the number of physical entities used for the HLT: ATLAS has designed an explicit Lvl-2 farm that provides an intermediate rejection after the Lvl-1 trigger and before the events are directed to the second farm for the Lvl-3 selection. CMS is based on a single farm running a single program that provides the full selection.

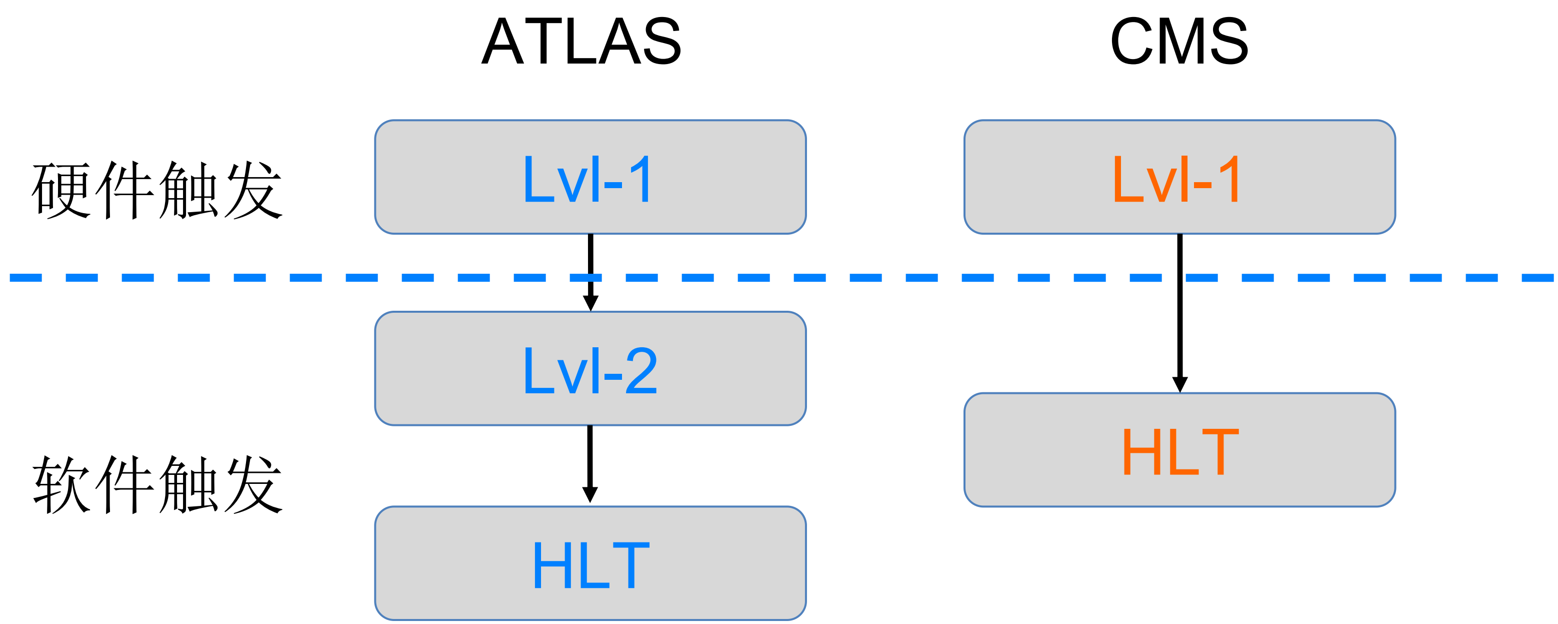

HLT：大规模商用PC搭建计算集群

触发效率比较

TABLE 14 Efficiency for triggering on fiducial electrons and muons in ATLAS and CMS

Object	ATLAS	CMS
Electrons	$E_T > 25$ GeV	$E_T > 29$ GeV
-Lvl-1 efficiency	95%	95%
-HLT efficiency	80%	77%
Muons	$P_T > 20$ GeV	$P_T > 19$ GeV
-Lvl-1 efficiency	95%	95%
-HLT efficiency	90%	86%

The efficiencies quoted at the HLT do not correspond to the same purity (thus, the difference between the two experiments). The thresholds quoted correspond to the parameters used for physics studies by the two experiments. The actual values used will, of course, be determined from early data.

ATLAS探测器建造过程

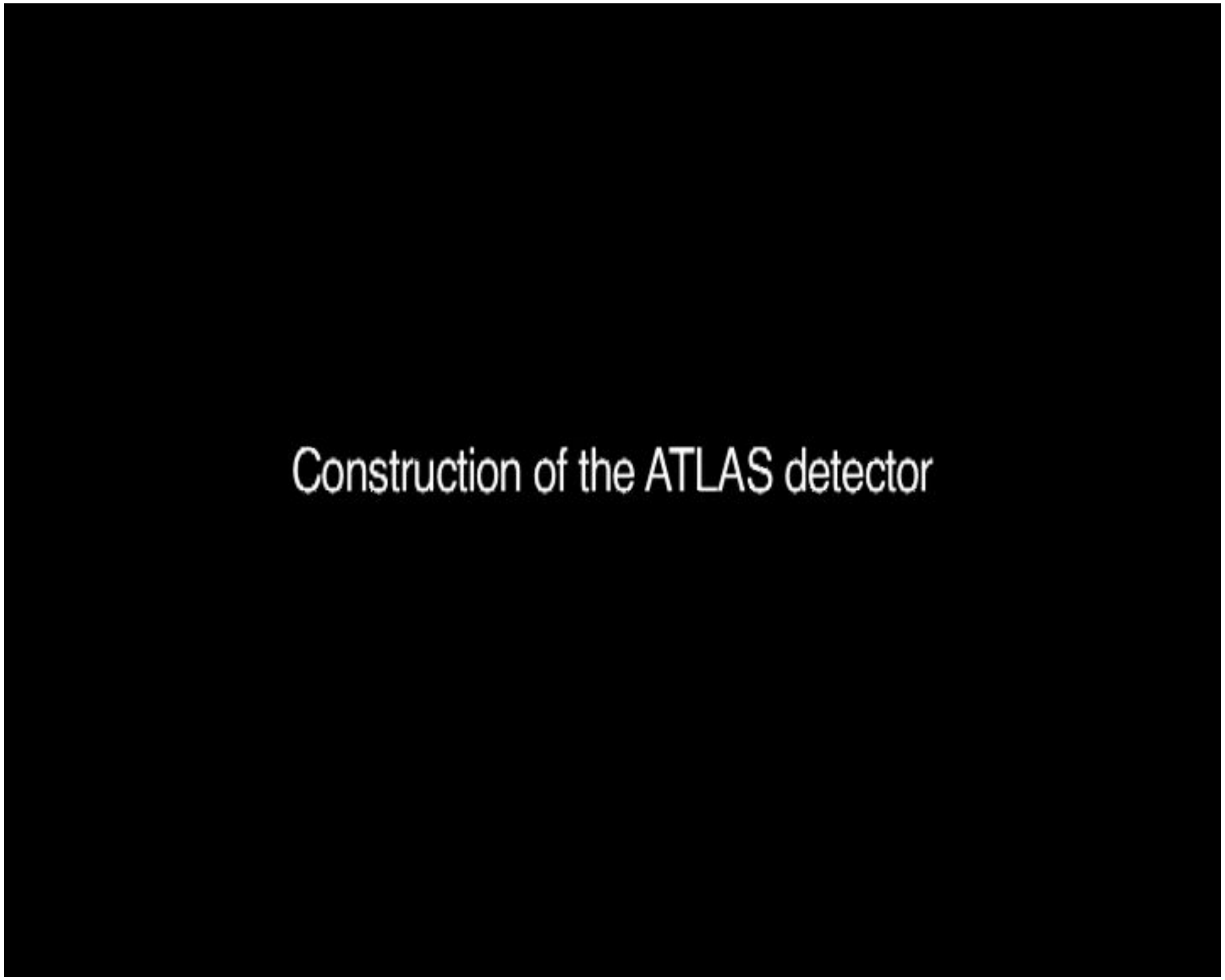

探测器到位时间

平均延期 ~2年

TABLE 15 Main construction milestones for the ATLAS and CMS detectors

	ATLAS		CMS	
Detector system	**TDR**	**Actual**	**TDR**	**Actual**
Pixels	06/03	03/07	03/05	12/07
Silicon microstrips (barrel)	12/02	07/05	03/04	10/06
Silicon microstrips (end caps)	12/02	06/06	03/04	10/06
Transition radiation tracker	03/04	12/05		
Electromagnetic calorimeter (barrel)	06/03	07/04	12/03	03/07
Electromagnetic calorimeter (end caps)	01/04	09/05	06/04	03/08
Hadronic calorimeter	12/02	02/04	12/03	12/04
Muon chambers	12/04	12/05	12/03	06/06
Solenoid magnet	01/02	09/01	03/03	12/05
Barrel toroid magnet	06/02	06/05		
End-cap toroid magnet	12/03	11/06		

Shown are the milestone dates for the delivery of major components to CERN, as planned in the Technical Design Reports (TDR), and the actual or future planned delivery of milestones.

ATLAS 探测器

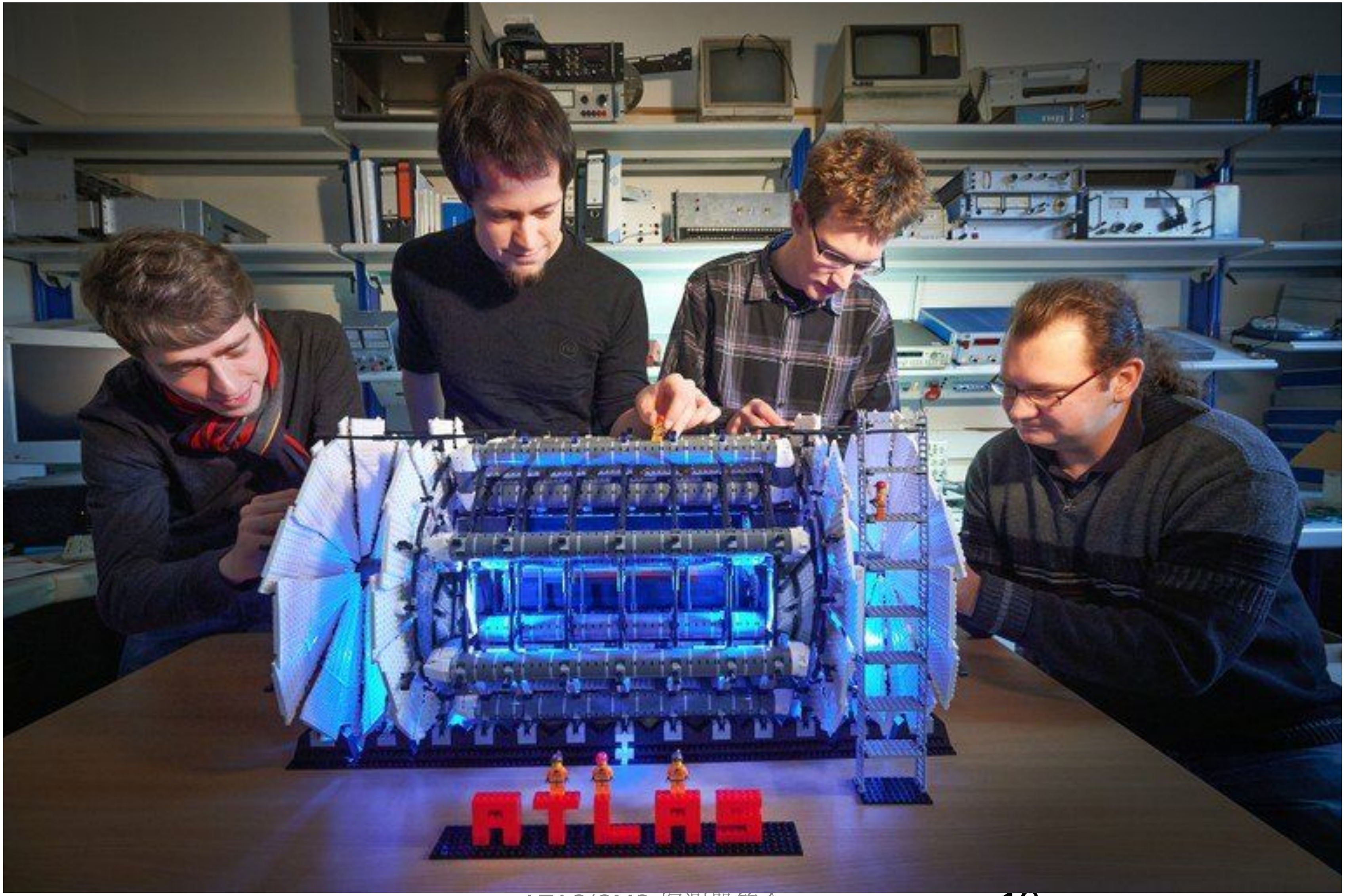

课程 II

径迹探测器系统

径迹探测

- 带电粒子与探测器作用，形成测量点（空间坐标）；由于磁场的存在，带电粒子以螺旋线方式出射。

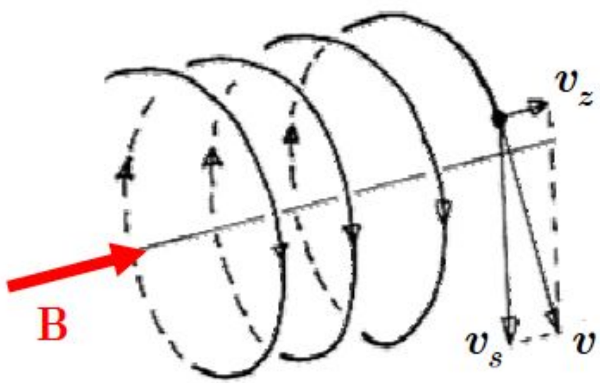

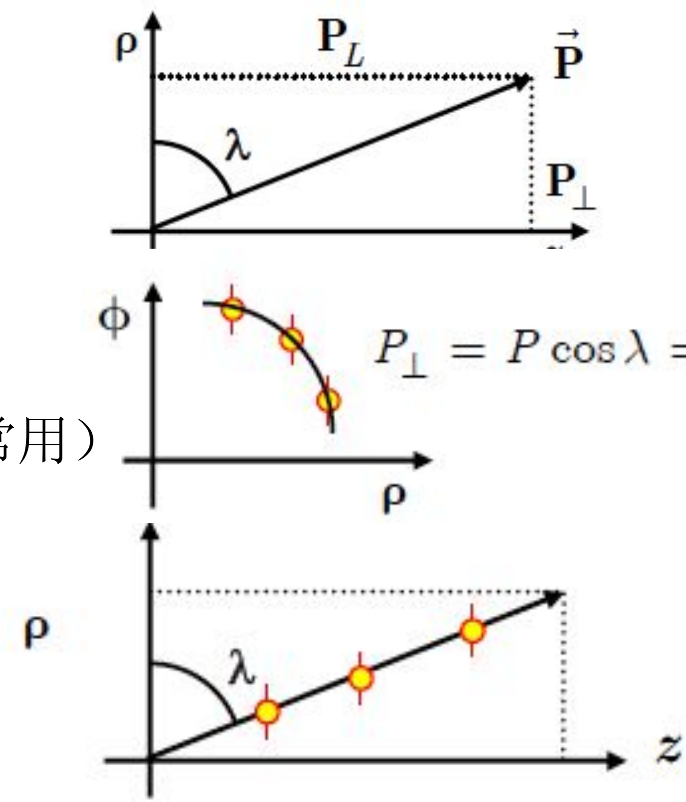

$$P_\perp = P\cos\lambda = 0.3BR$$

- R-Φ平面测量横动量（强子对撞器常用）

$$R(m) = \frac{P_T\ (\mathrm{GeV})}{0.3B\cdot(\mathrm{T})}$$

- R-z平面测角度

动量测量

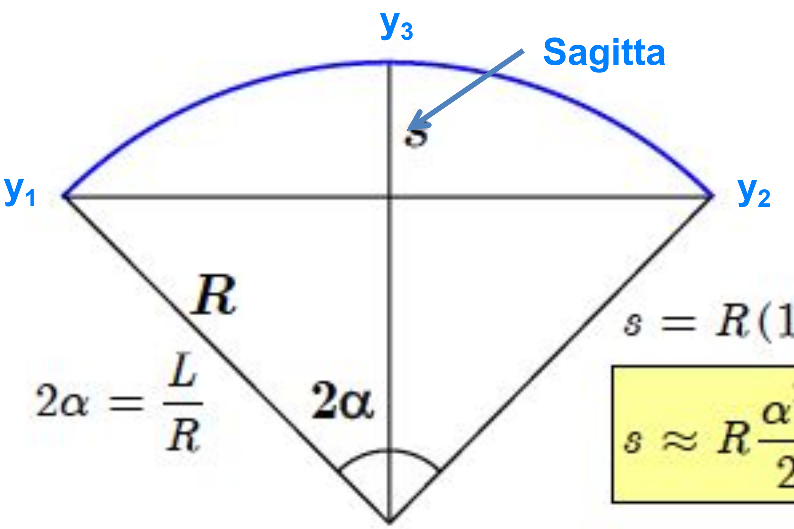

$$s = R(1 - \cos\alpha)$$

$$s \approx R\frac{\alpha^2}{2} = \frac{L^2}{8R}$$

$$s = y_3 - \frac{y_1 + y_2}{2} \qquad \delta s = \sqrt{\frac{3}{2}}\delta y \sim \delta y$$

$$R = \frac{p}{0.3B} \quad \text{and} \quad \frac{\delta p}{p} = \frac{\delta R}{R}$$

$$\delta s = \frac{L^2}{8R}\frac{\delta R}{R} \sim \delta y \quad \rightarrow \quad \frac{L^2}{8R}\frac{\delta p}{p} \sim \delta y$$

- 动量测量相对精度依赖于：
  - 正比于粒子动量 ***p***
  - 反比于磁场强度 ***B***
  - 反比于径迹长度 ***L^2***
  - 正比于测量点分辨率 ***δy***
- 探测器设计需要平衡各种指标

$$\frac{\delta p}{p} = \frac{8R}{L^2}\delta y \quad \sim \quad \frac{\delta p}{p} = \frac{8p}{0.3BL^2}\delta y$$

径迹探测器主要考虑

1. Robust and redundant pattern recognition, providing efficient and precise measurements of the trajectories of all charged particles with transverse momentum above 1 GeV within the geometrical acceptance. 粒子寻迹
2. High-level triggering capabilities for electrons, muons, τ leptons, and b jets. **HLT触发**
3. Precise measurements of secondary vertices and of impact parameters for efficient identification of heavy flavors (b jets and exclusive B-hadron decays in particular). 次级顶点重建 & 重味夸克标记
4. Identification of electrons through matching of tracks to clusters in the ECAL, matching of reconstructed track momentum to reconstructed energy in the ECAL, and the use of specific technologies (transition radiation in the ATLAS TRT). 电子甄别
5. Identification and measurements of hadronic decays of τ leptons in both one-prong and three-prong decay topologies. **Tau轻子甄别**

径迹探测器总体性能

TABLE 7 Main performance characteristics of the ATLAS and CMS trackers

	ATLAS	CMS
Reconstruction efficiency for muons with $p_T = 1$ GeV	96.8%	97.0%
Reconstruction efficiency for pions with $p_T = 1$ GeV	84.0%	80.0%
Reconstruction efficiency for electrons with $p_T = 5$ GeV	90.0%	85.0%
Momentum resolution at $p_T = 1$ GeV and $\eta \approx 0$	1.3%	0.7%
Momentum resolution at $p_T = 1$ GeV and $\eta \approx 2.5$	2.0%	2.0%
Momentum resolution at $p_T = 100$ GeV and $\eta \approx 0$	3.8%	1.5%
Momentum resolution at $p_T = 100$ GeV and $\eta \approx 2.5$	11%	7%
Transverse i.p. resolution at $p_T = 1$ GeV and $\eta \approx 0$ (μm)	75	90
Transverse i.p. resolution at $p_T = 1$ GeV and $\eta \approx 2.5$ (μm)	200	220
Transverse i.p. resolution at $p_T = 1000$ GeV and $\eta \approx 0$ (μm)	11	9
Transverse i.p. resolution at $p_T = 1000$ GeV and $\eta \approx 2.5$ (μm)	11	11
Longitudinal i.p. resolution at $p_T = 1$ GeV and $\eta \approx 0$ (μm)	150	125
Longitudinal i.p. resolution at $p_T = 1$ GeV and $\eta \approx 2.5$ (μm)	900	1060
Longitudinal i.p. resolution at $p_T = 1000$ GeV and $\eta \approx 0$ (μm)	90	22–42
Longitudinal i.p. resolution at $p_T = 1000$ GeV and $\eta \approx 2.5$ (μm)	190	70

ATLAS 径迹探测器

- 由内向外：PIXEL（硅像素）、SCT（硅微条）及TRT（跃迁辐射），测量精度从高到低（靠近对撞点粒子密度高，需要高空间分辨率区分，降低探测器占有率）

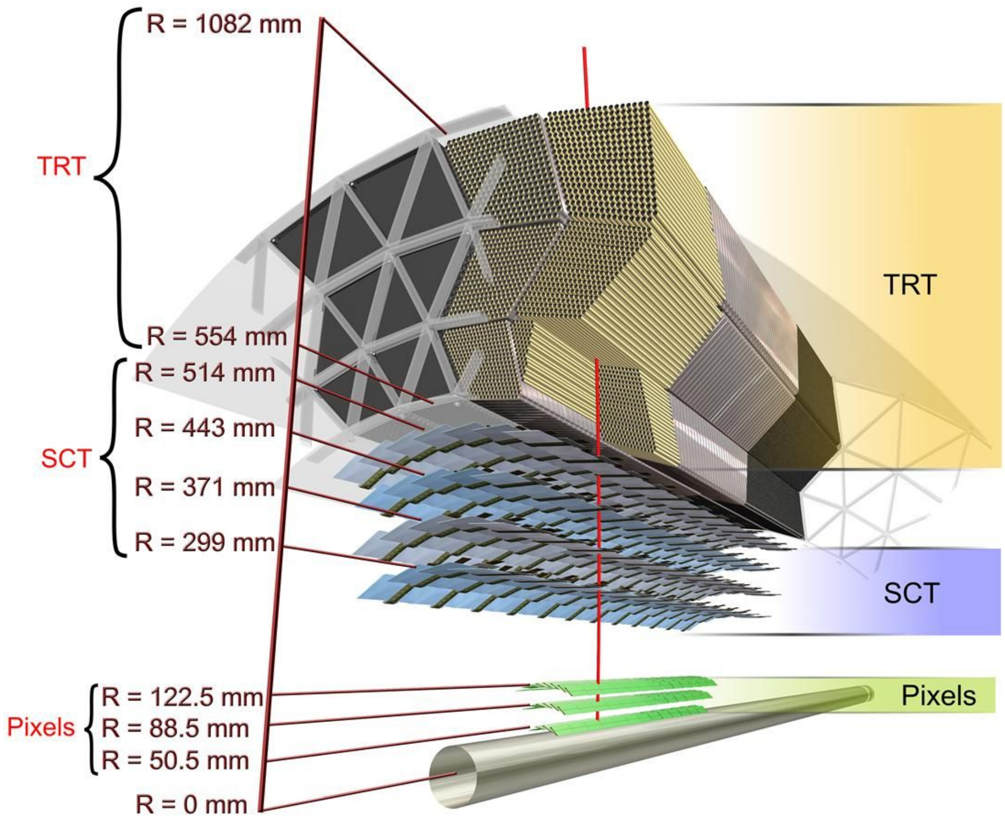

TRT：数十个测量点有利于寻迹（精度低于硅微条），电子甄别能力，造价低（相对于硅探测器）

PIXEL及**SCT**均为硅探测器，靠近对撞点，精度高、抗辐照

CMS 径迹探测器

- 仅有硅像素和硅微条探测器构成，最大的硅探测器

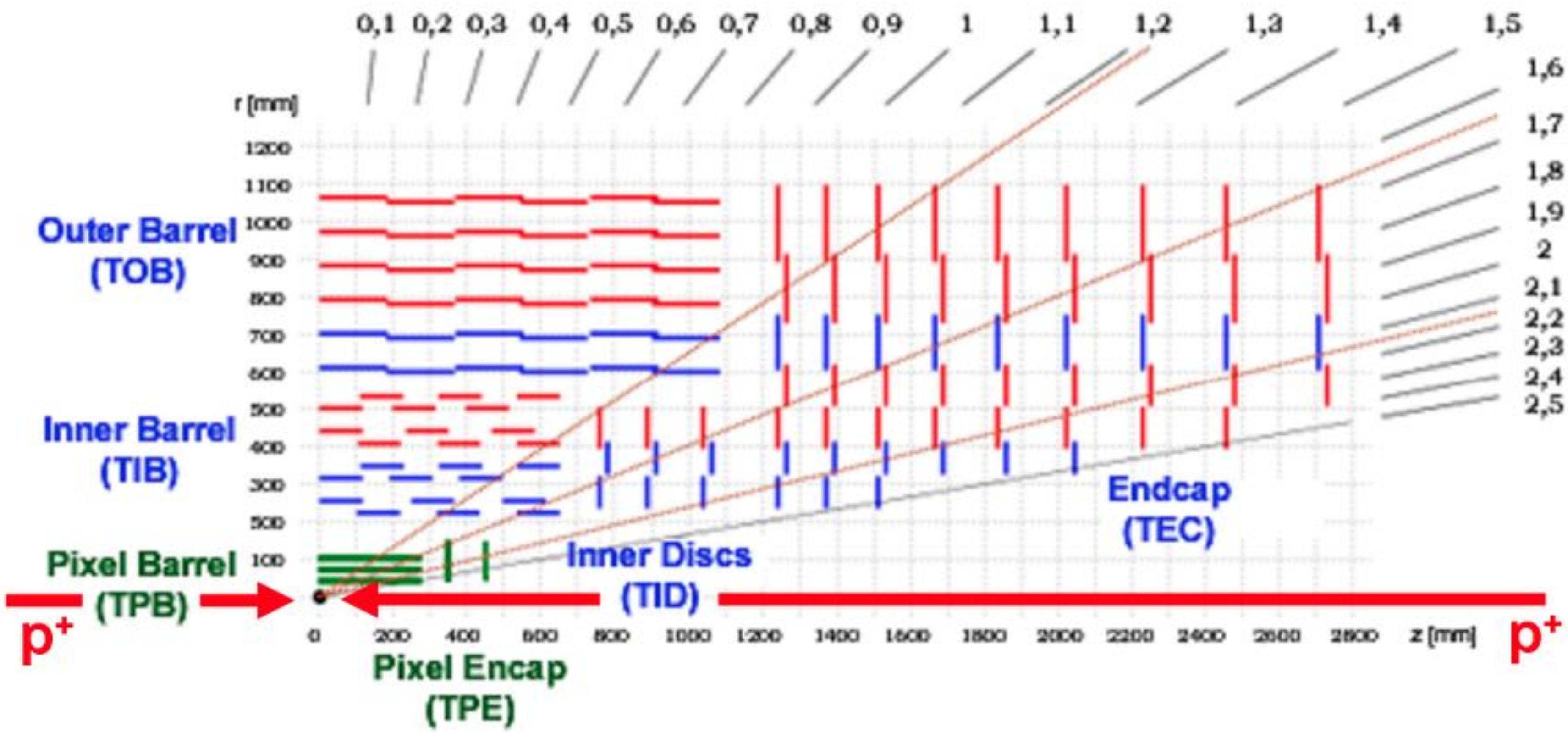

PIXEL 探测器

初级碰撞顶点重建

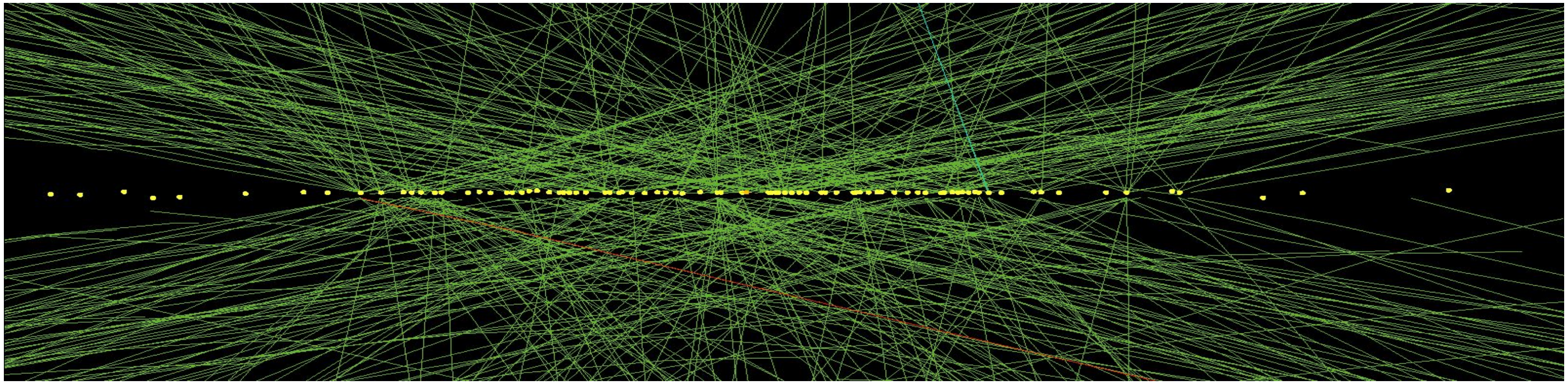

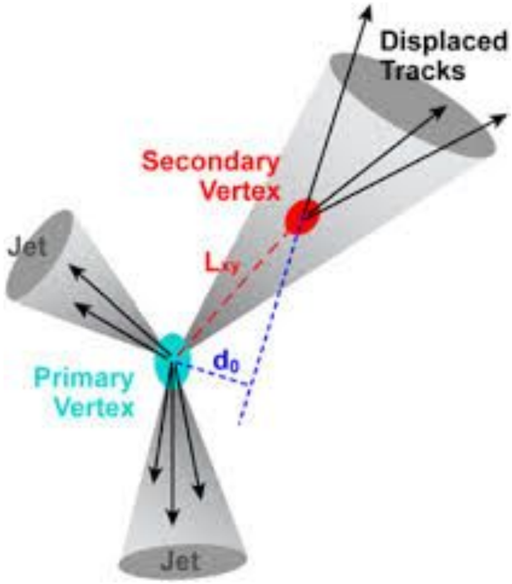

次级碰撞顶点重建

↓

b-tagging

ATLAS / CMS PIXEL

TABLE 6 Main parameters of the ATLAS and CMS pixel systems

	ATLAS	CMS
Number of hits per track	3	3
Total number of channels	80 10^6	66 10^6
Pixel size (µm in $R\phi$ × µm in z/R)	50 × 400	100 × 150
Lorentz angle (degrees), initial to end	12 to 4	26 to 8
Tilt in $R\phi$ (degrees)	20 (only barrel)	20 (only end cap)
Total active area of silicon (m^2)	1.7 (n^+/n)	1.0 (n^+/n)
Sensor thickness (µm)	250	285
Total number of modules	1744 (288 in disks)	1440 (672 in disks)
Barrel layer radii (cm)	5.1, 8.9, 12.3	4.4, 7.3, 10.2
Disk layer min. to max. radii (cm)	8.9 to 15.0	6.0 to 15.0
Disk positions in z (cm)	49.5, 58.0, 65.0	34.5, 46.5
Signal-to-noise ratio for minimum ionizing particles (day 1)	120	130
Total fluence at L = 10^{34} (n_{eq}/cm^2/year) at radius of 4–5 cm (innermost layer)	3×10^{14}	3×10^{14}
Signal-to-noise ratio (after 10^{15} n_{eq}/cm^2)	80	80
Resolution in $R\phi$ (µm)	≈10	≈10
Resolution in z/R (µm)	≈100	≈20

硅像素探测器

- ATLAS和CMS均采用**复合式硅像素探测器**：传感器与前端电子学ASIC芯片通过倒装焊（Bump-Bonding）连接。

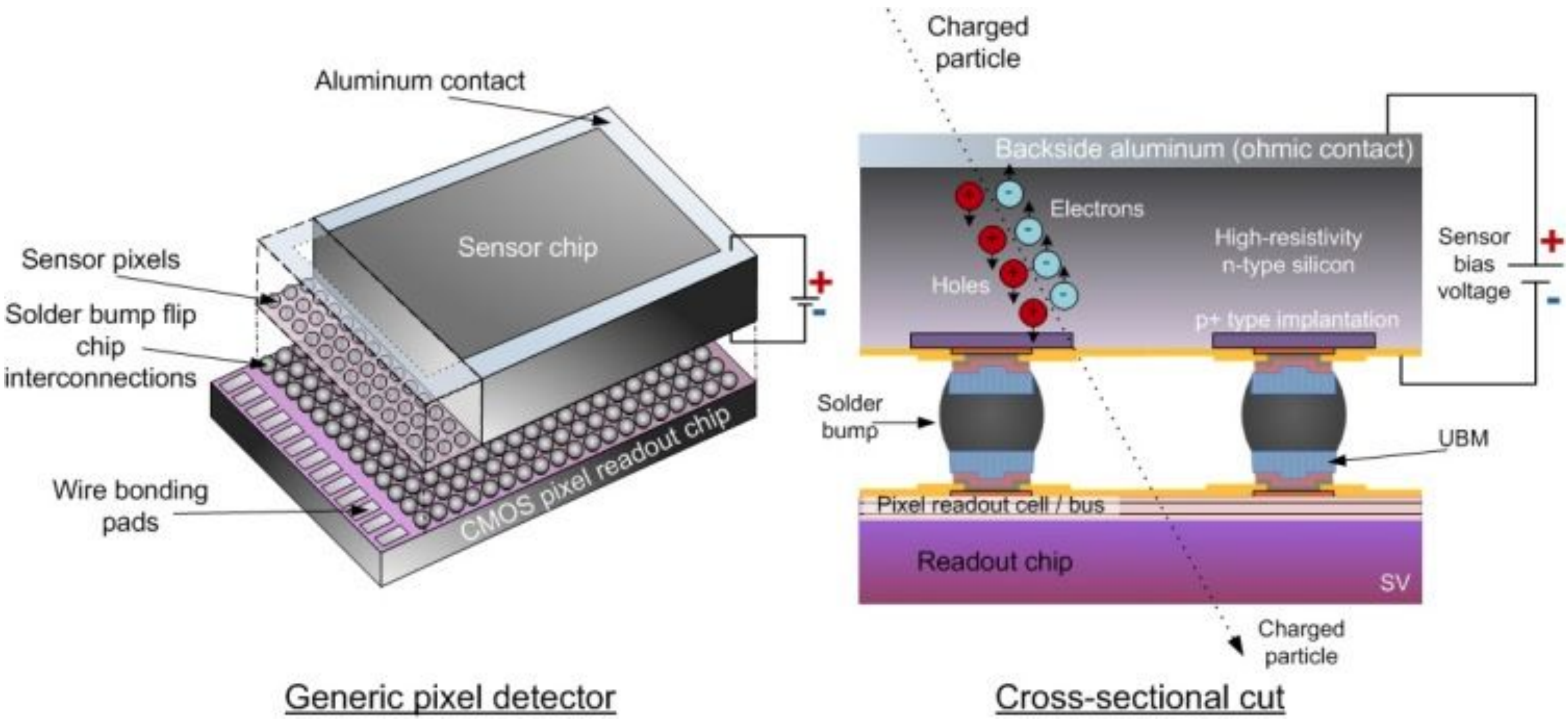

ATLAS/ CMS 硅像素探测器模块

- 硅像素探测器模块为最基本单元

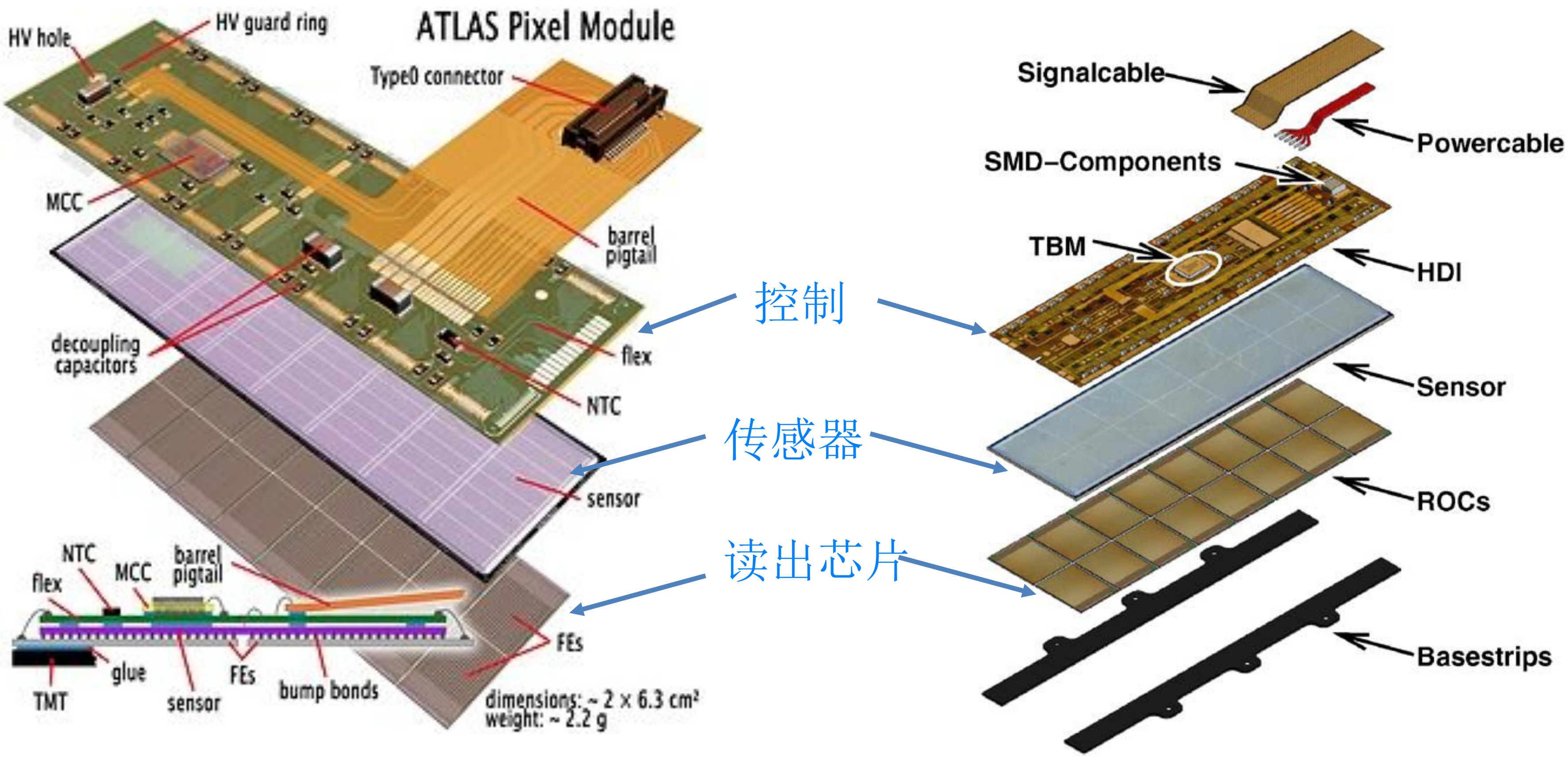

硅像素传感器（Pixel Sensor）

- n^+-on-n 平面式硅像素传感器基于特种工艺，像素尺寸50×400 (100×150) μm²， 抗辐照

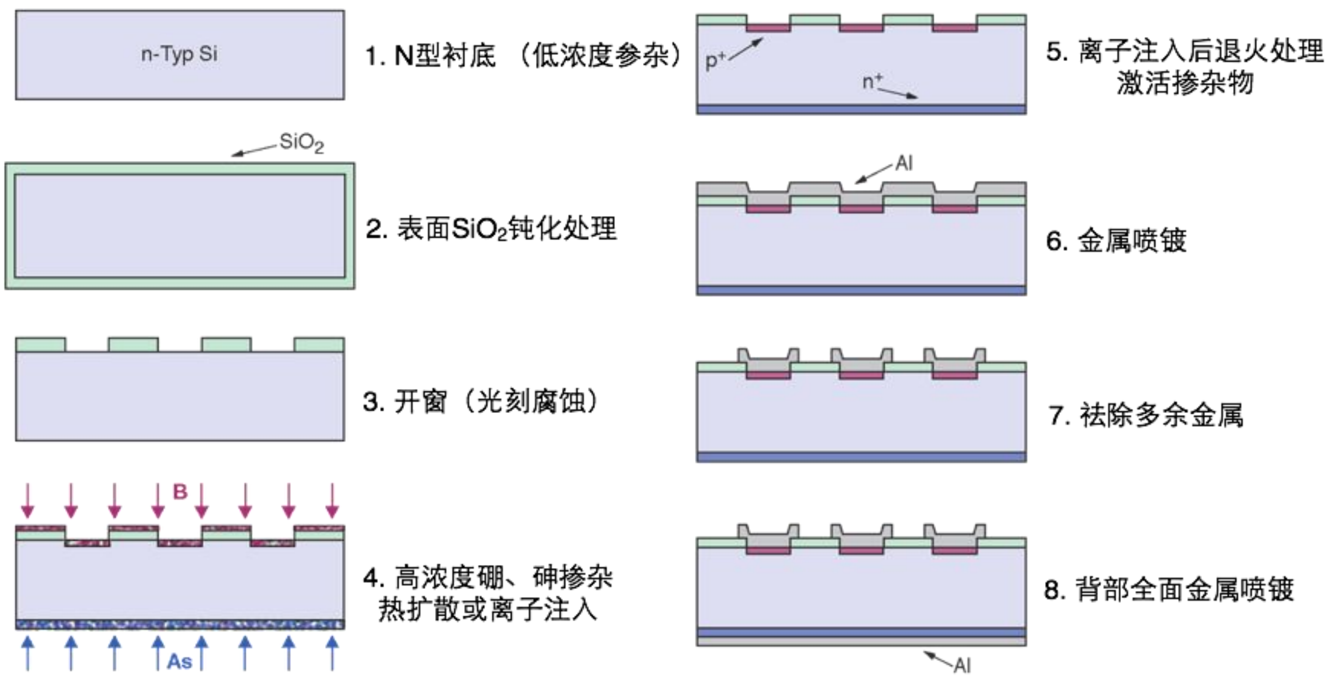

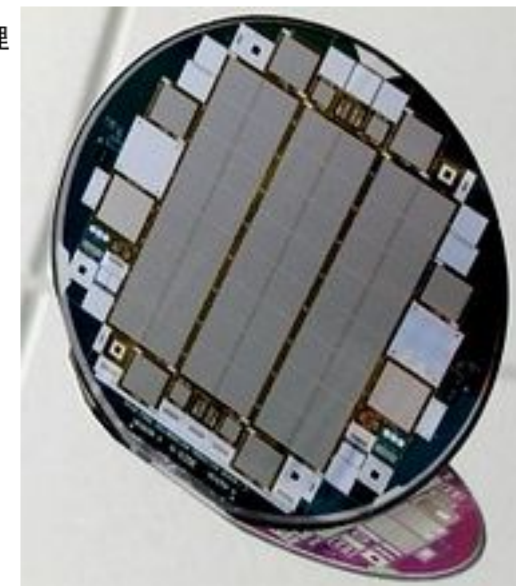

前端读出电子学

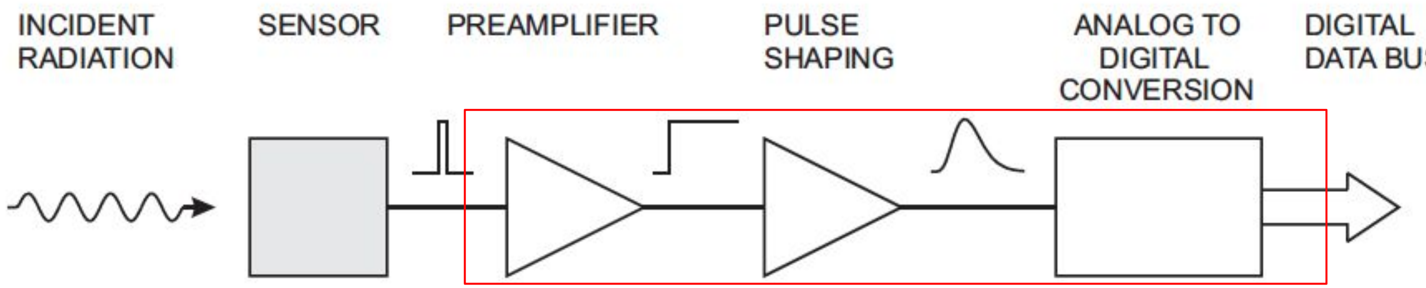

- 基于250 nm CMOS工艺，深亚微米（Deep Sub-Micron），数模混合电路，具备抗辐照性能。

ATLAS 读出芯片FE-I3
逻辑框图

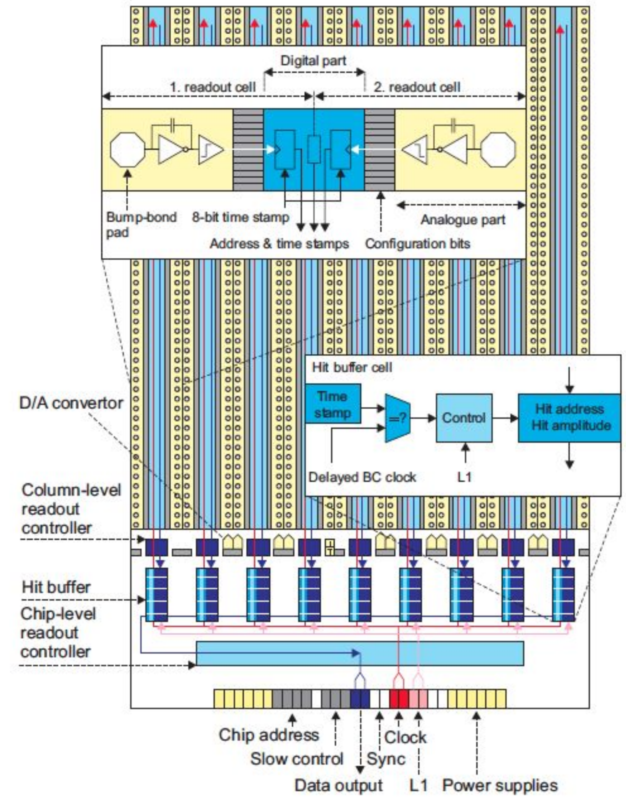

CMOS工艺

Table 3. Summary of the ATLAS pixel front-end chips designed and fabricated as described in the text. The chips contain two (2M), three (3M) or six (6M) metal layers as indicated.

Chip	Year	Cell size [μm^2]	Col × Row	Transis-tors	Technology	References
Beer & Pastis	1996	50×436	12×63	–	AMS 0.8μm BiCMOS, 2M	[6, 9]
M72b	1997	50×536	12×64	–	HP 0.8μm CMOS, 2M	[6]
Marebo	1997	50×397	12×63	0.1 M	DMILL 0.8μm BiCMOS, 2M	[7, 8]
FE-B	1998	50×400	18×160	0.8 M	HP 0.8μm CMOS, 3M	[10 – 12]
FE-A/C	1998	50×400	18×160	0.8 M	AMS 0.8μm BiCMOS, 2M	[9, 12]
FE-D1	1999	50×400	18×160	0.8 M	DMILL 0.8μm BiCMOS, 2M	[12]
FE-D2	2000	50×400	18×160	0.8 M	DMILL 0.8μm BiCMOS, 2M	–
FE-I1	2002	50×400	18×160	2.5 M	DSM 0.25μm CMOS, 6M	[13]
FE-I2/I2.1	2003	50×400	18×160	3.5 M	DSM 0.25μm CMOS, 6M	[14]
FE-I3	2003	50×400	18×160	3.5 M	DSM 0.25μm CMOS, 6M	[15 – 18]

- 要求工艺具备抗辐照性能，其生产线应在探测器研制直至建造周期内稳定。

硅像素探测器升级

- 传感器升级考虑（抗更强辐照）：平面式改进型，3D 传感器以及CMOS传感器等

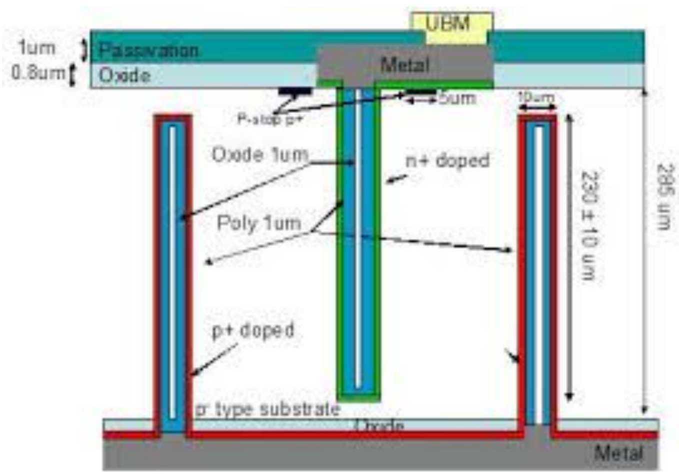

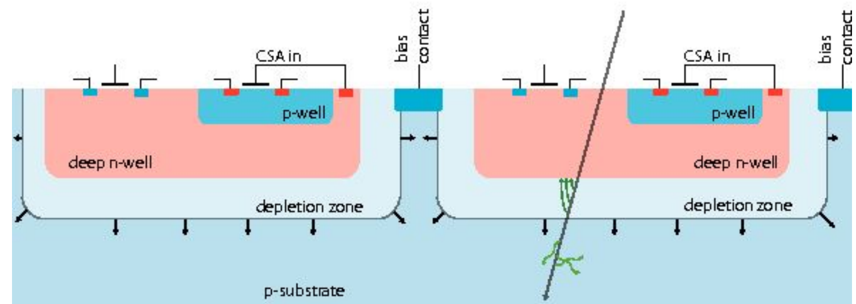

- 读出电子学：更小尺寸的深亚微米CMOS制程 → RD53合作组（ATLAS、CMS、CLIC 等）基于TSMC 65nm 工艺，共同开发功能模块。3D集成也有尝试，但是尚不成熟。

ATLAS / CMS STRIPS

- ATLAS / CMS 采用硅微条探测器作为径迹探测器主体，可以提供多个高精度的测量点。

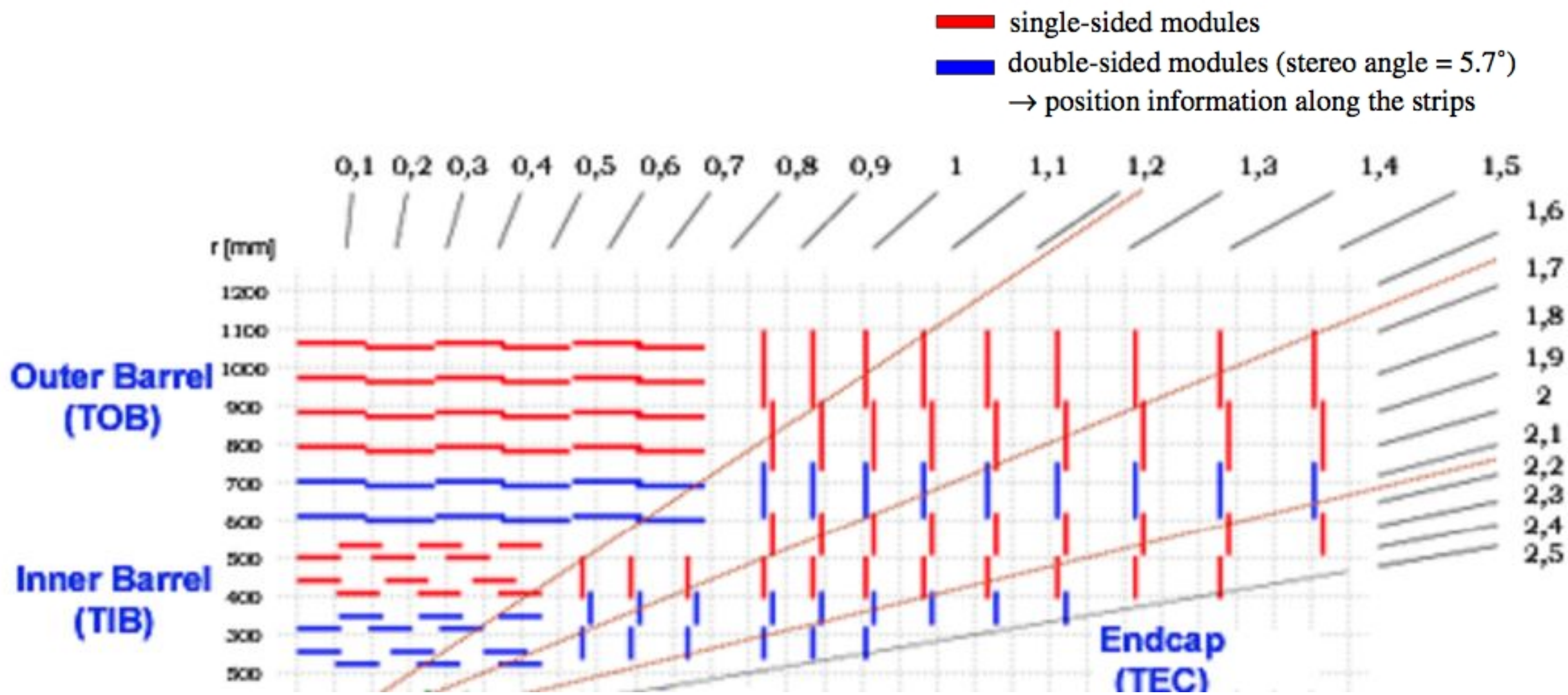

硅微条传感器

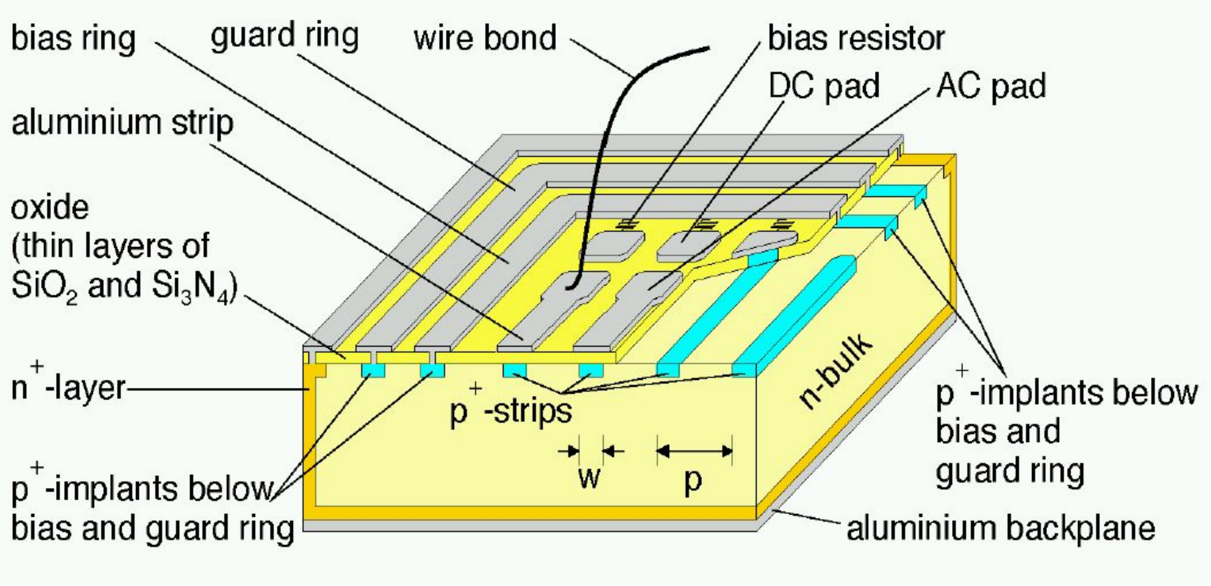

- Single-sided sensors with p^+-type strips in an n-type bulk
- 6" wafer technology (Atlas: 4")
- AC-coupled readout
- Pitch ranges from 80-210μm
- Constant width/pitch (→ constant strip capacitance)
- Readout strip and guard ring geometries optimised to increase breakdown voltage

读出电子学

- 读出ASIC芯片：ABCD（ATLAS）和APV25（CMS），基于深亚微米CMOS工艺。ATLAS采用二进制输出（击中1，没击中0），CMS采用模拟输出，尽可能保留信号。后者对相同信号可以实现更高分辨率，但是需要更高带宽，信号刻度复杂。

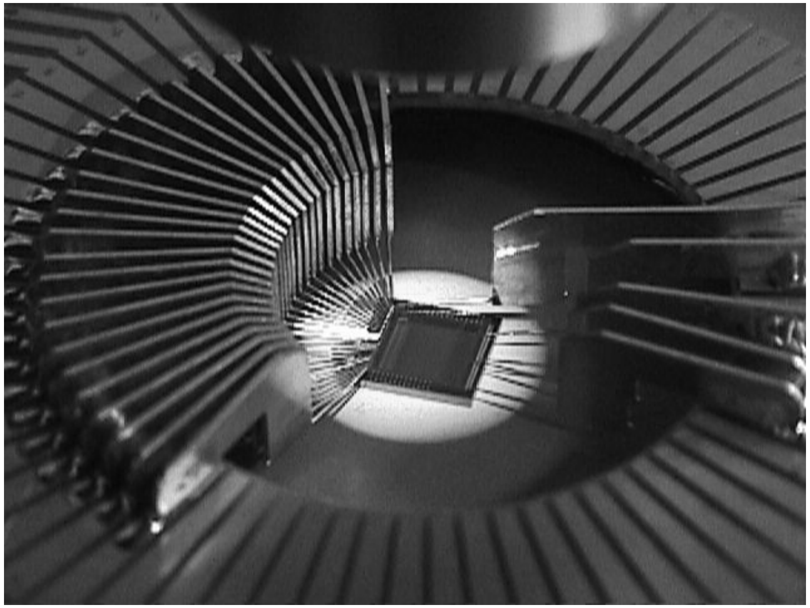

APV25 功能十分丰富，在其它探测器（例如气体探测器）读出中也有使用

硅微条探测器模块

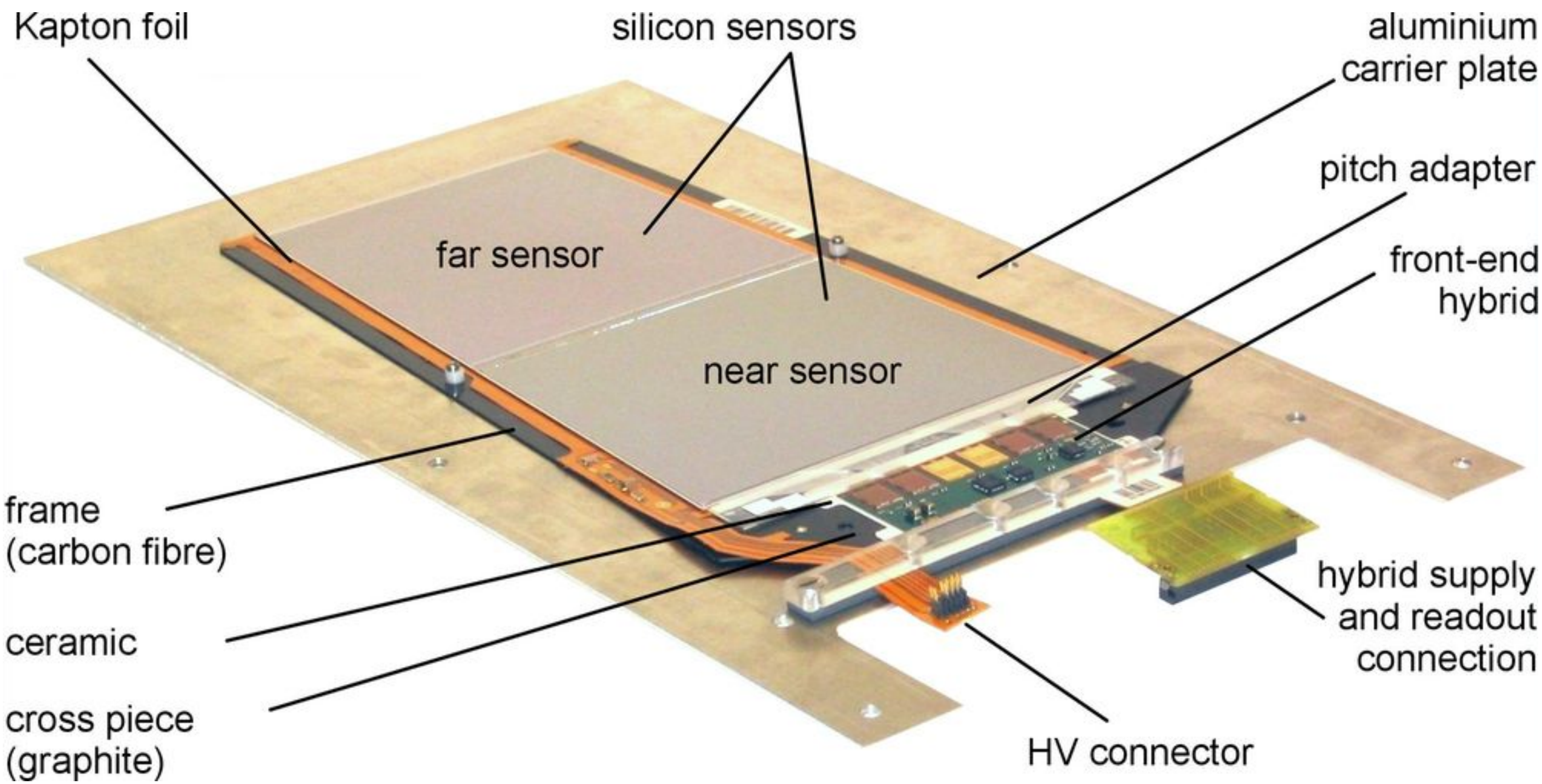

Kapton foil
silicon sensors
aluminium carrier plate
pitch adapter
front-end hybrid
far sensor
near sensor
frame (carbon fibre)
ceramic
cross piece (graphite)
hybrid supply and readout connection
HV connector

ATLAS 径迹探测器

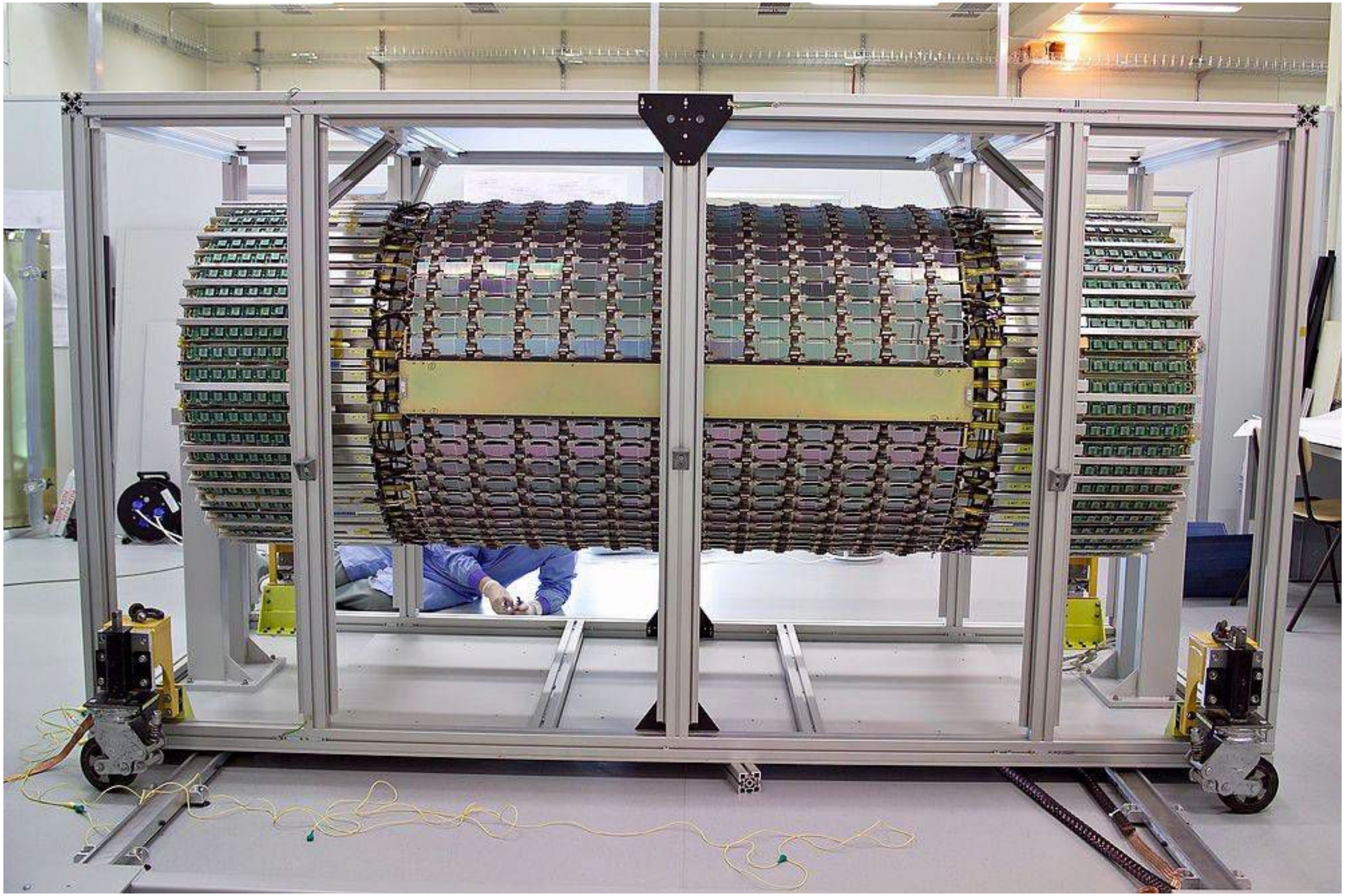

CMS 径迹探测器

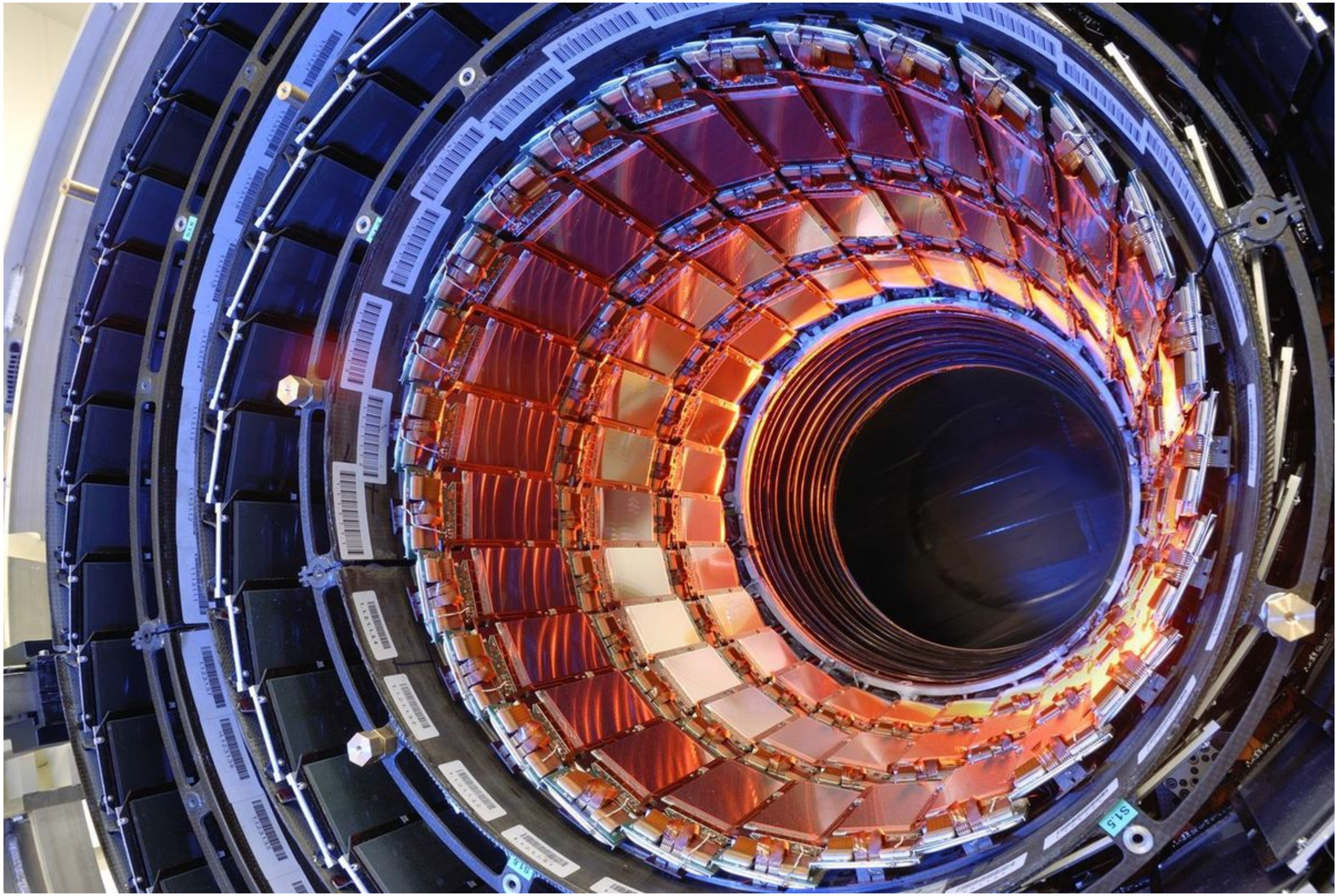

硅微条探测器升级

- 现有硅微条传感器通过改进设计，提高抗辐照性能；或是基于CMOS工艺设计硅微条传感器（ATLAS），内置部分电路，简化读出芯片功能，减少打线数量。

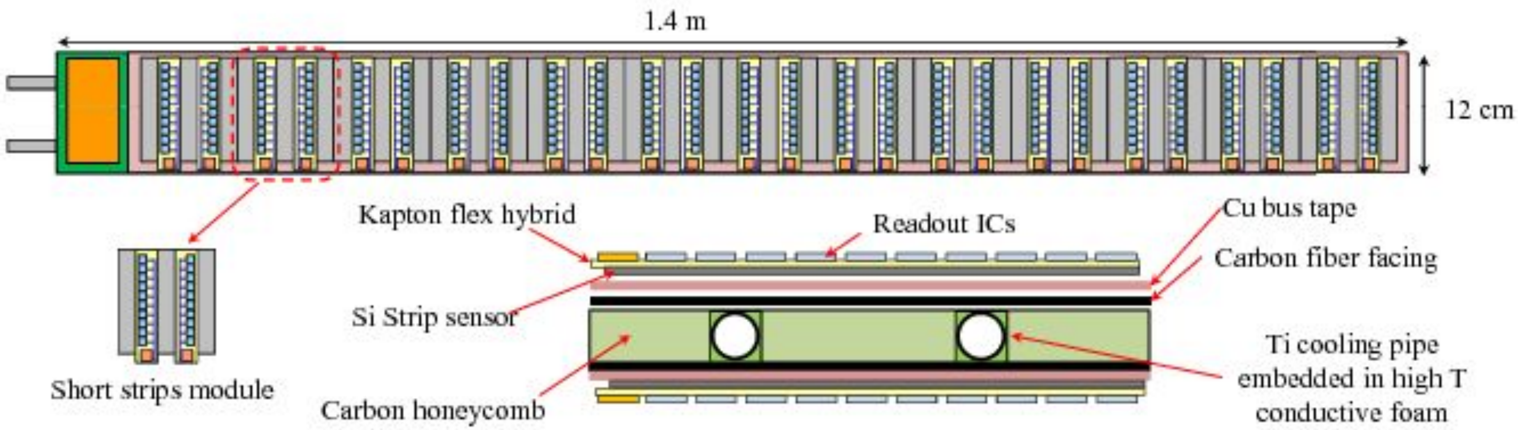

- 读出芯片采用更小尺寸（130 nm甚至65 nm CMOS工艺），提升性能（复杂功能、低功耗），抗辐照等。

ATLAS TRT探测器

- 能够以经济的方式（相对于硅探测器）提供多个测量点；此外还可以通过跃迁辐射（Transition Radiation），提供e/π甄别。

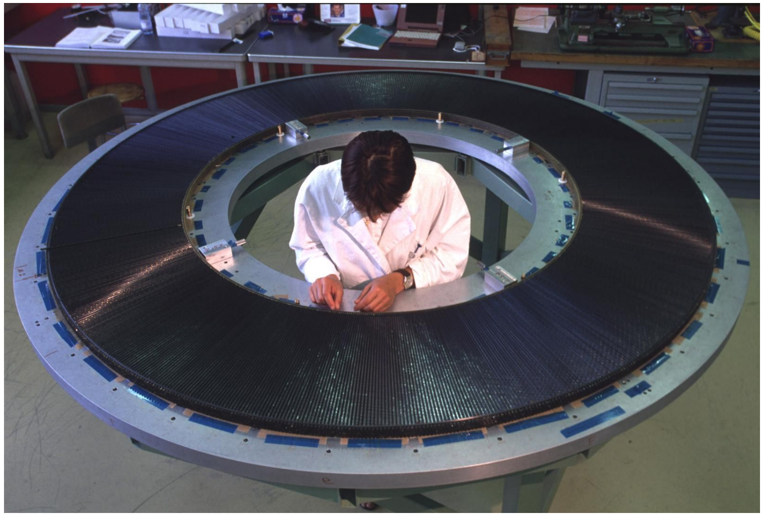

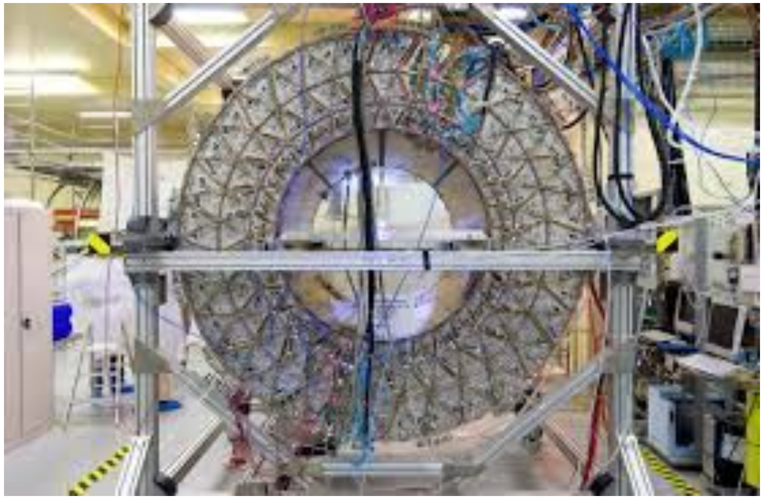

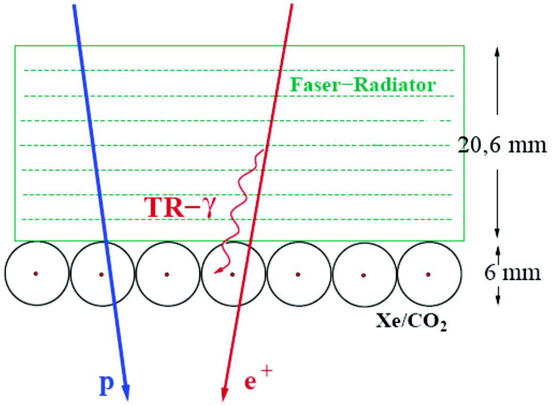

电子穿过时发射跃迁辐射光子

径迹探测器物质量分布

- 由于多次粒子散射效应，径迹探测器要求尽量降低物质量。

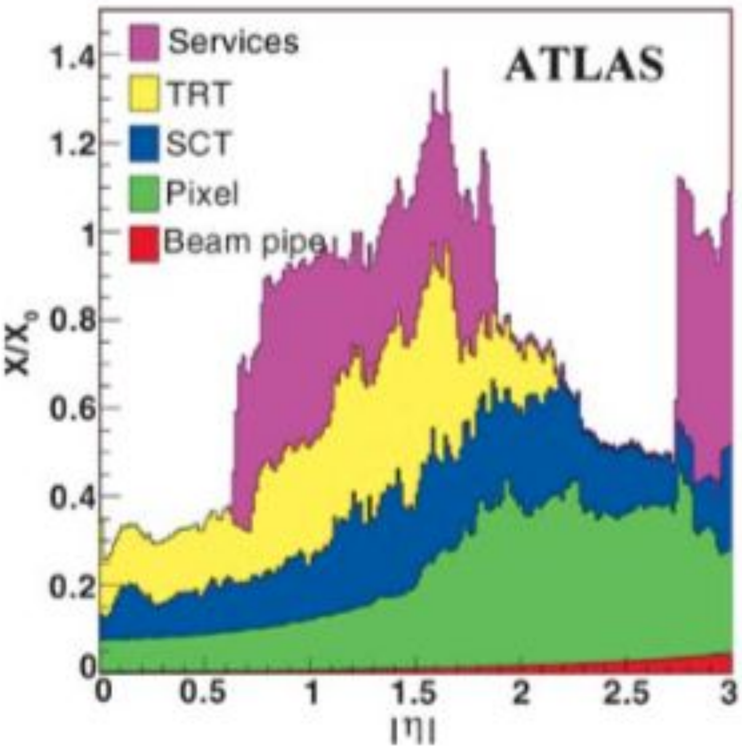

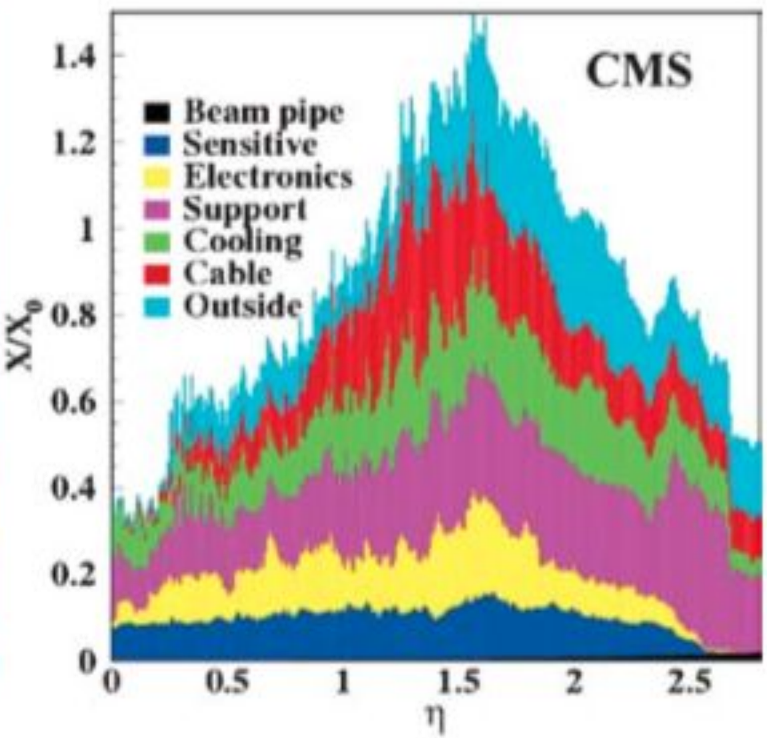

物质量：现实与理想

TABLE 5 Evolution of the amount of material expected in the ATLAS and CMS trackers from 1994 to 2006

Date	ATLAS $\eta \approx 0$	$\eta \approx 1.7$	CMS $\eta \approx 0$	$\eta \approx 1.7$
1994 (Technical Proposals)	0.20	0.70	0.15	0.60
1997 (Technical Design Reports)	0.25	1.50	0.25	0.85
2006 (End of construction)	0.35	1.35	0.35	1.50

- 设计初期，很容易低估径迹探测器物质量：支撑结构、电缆、冷却结构等；
- 探测器开始运行前，需要完整测量/估计物质量；运行后，可以利用实验数据确定物质量，甚至是结构细节。

测量物质量分布

- 可以使用X-光扫描的方法初步测量物质量分部，然后通过重建强子作用或是转换光子的方法，准确测量物质量。

Hadronic Interactions

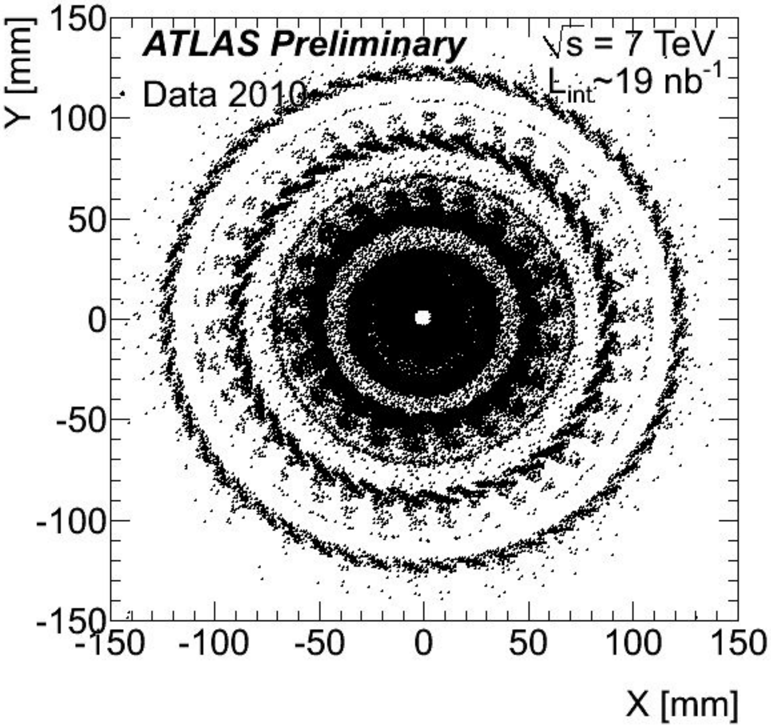

Photon Conversions

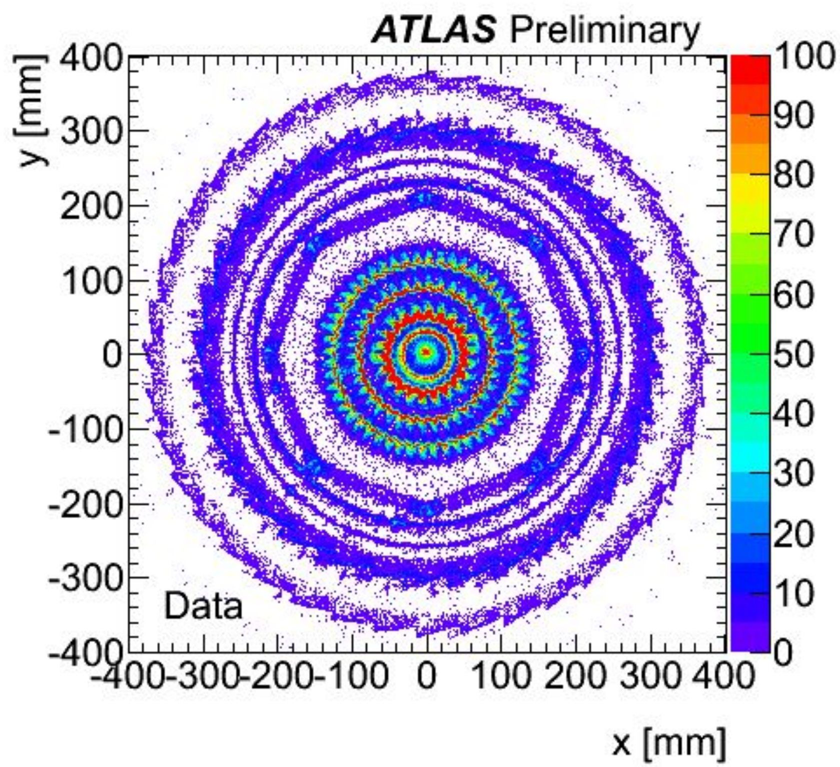

探测器调准（Alignment）

•机械调准：通过精确的机械设计及安装，通常可以实现毫米量级的位置精度；再使用频率扫描干涉（FSI）方法，实现10微米量级的位置精度。

•径迹调准：通过重建径迹，根据其残差（Residual）来进一步修正探测器部件的位置信息，精度可至几个微米。

课程 III

量能器系统

系统考虑要点

课程 IV

缪子探测器系统